

Tract-based parameterization of local white matter geometry

P. Savadjiev¹, M. Kubicki¹, S. Bouix¹, G. L. Kindlmann², M. E. Shenton^{1,3}, and C-F. Westin⁴

¹Psychiatry, Brigham and Women's Hospital, Harvard Medical School, Boston, MA, United States, ²Computer Science, University of Chicago, Chicago, IL, United States, ³Psychiatry, VA Boston Healthcare System, Brockton, MA, United States, ⁴Radiology, Brigham and Women's Hospital, Harvard Medical School, Boston, MA, United States

Introduction A set of scalar measures was recently introduced in [1,2] to describe the geometrical properties of white matter directly from diffusion tensor fields. Here we build on this work by constructing parametric representations of white matter fibre clusters and by examining the behavior of the geometric indices along the tract parameterization. Tractography is used only to define the parameterization framework. As described in [1,2], the scalar geometric indices are computed independently of tractography and its potential drawbacks. Measures of fibre geometry and its variation along tracts can be useful in the study of normal white matter development, and also of diseases that may affect it, e.g. as indicators of neurodegenerative processes. This study is therefore a first step towards building a tract-based geometric analysis method for evaluating white matter in healthy and pathological populations.

Theory The scalar indices of white matter dispersion and curving presented in [1,2] are obtained via a differential analysis of the diffusion tensor field, with a focus on tensor orientation. Their definition is based on the *rotation tangents* Φ_i , $i \in \{1,2,3\}$, introduced in [3] as a basis for describing variation in tensor orientation within a diffusion tensor field. Their projection on the gradient of the diffusion tensor field ∇F results in three spatial gradients of orientation $\nabla\phi_i = \Phi_i : F$, which indicate in \mathbf{R}^3 the direction of largest variation of tensor orientation around tensor eigenvector \mathbf{e}_i [3]. The three $\nabla\phi_i$ vectors are then projected onto the three tensor eigenvectors, in order to obtain nine different projections of the form $\nabla\phi_i \cdot \mathbf{e}_j$, $i,j \in \{1,2,3\}$, each of which will have a high value for a specific local geometrical configuration of the tensor field. Appropriate projections are then combined to define a scalar measure of fibre dispersion, \mathcal{D} , and a scalar measure of fibre curving, C , such that $C = ((\nabla\phi_2 \nabla\phi_2^T + \nabla\phi_3 \nabla\phi_3^T) : (\mathbf{e}_1 \mathbf{e}_1^T))^{1/2}$ and $\mathcal{D} = ((\nabla\phi_2 \nabla\phi_2^T + \nabla\phi_3 \nabla\phi_3^T) : (\mathbf{e}_2 \mathbf{e}_2^T + \mathbf{e}_3 \mathbf{e}_3^T))^{1/2}$.

Methods Diffusion-weighted images (DWI) were acquired on a GE Signa HDxt 3.0T scanner using an echo planar imaging sequence with a double echo option, an 8 Channel coil and ASSET with a SENSE-factor of 2. The acquisition consisted in 51 directions with $b=900$ s/mm², and 8 images with $b=0$ s/mm². The scan parameters were: TR=17000 ms, TE=78 ms, FOV=24 cm, 144×144 encoding steps, 1.7 mm slice thickness. A total of 85 axial slices covering the whole brain were acquired. Diffusion tensors were reconstructed from the DWI using a weighted least-squares approach (e.g. [4]), and were normalized by dividing each tensor by its norm [3], in order to remove any effect of tensor size on the computed indices [1,2]. The dispersion and curving indices were then computed at each voxel where the linear measure of anisotropy [4] was above 0.1. For the purposes of tract-based analysis, standard streamline tractography [5] was run starting with a small seed region in the splenium of the corpus callosum. The resulting tracts are visualized in Fig. 1, colored by the geometric indices. Two representative fibres were manually selected as cluster centers (shown in Fig. 1), and the method of [6] was used to group the fibres into two clusters, based on similarity with the cluster center. Based on [6], the cluster centers were then parameterized by normalized arc length s ($0 \leq s \leq 1$), and the mean and standard deviation of each geometric index over the cluster was computed and mapped along the parameterization, with results presented in Fig. 2.

Results The following results are relative to two clusters of the posterior fibres of the corpus callosum, shown in Fig. 1. Cluster 1 consists of fibres projecting to the parietal cortex, and cluster 2 is made of fibres projecting to the temporal lobe.

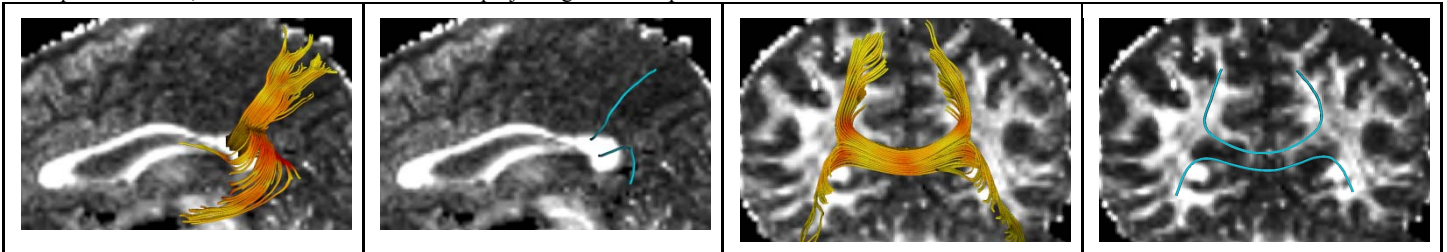


Figure 1. Left to right: a sagittal view of the fibres colored by dispersion \mathcal{D} , with red indicating high index value; the two cluster centers colored in blue; a coronal view of the fibres colored by curving C , also with red indicating high index value; the cluster centres. The fractional anisotropy (FA) image is shown in the background.

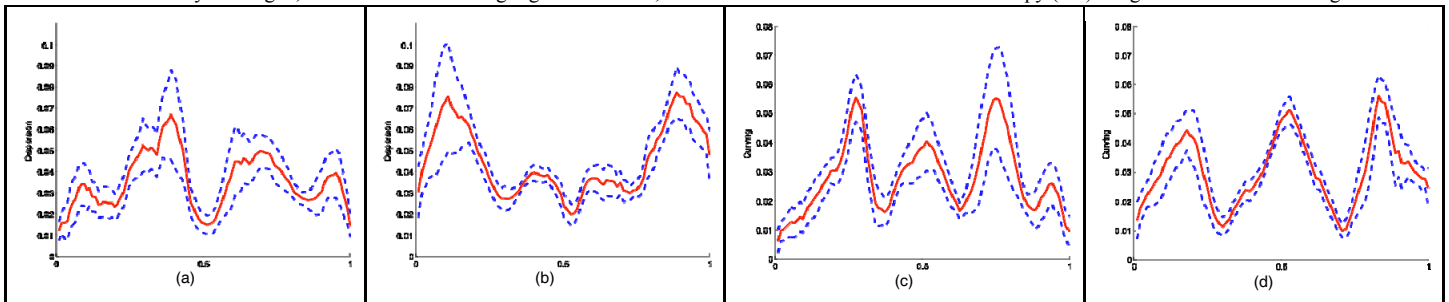


Figure 2. (a) Dispersion \mathcal{D} mapped along the parameterization of cluster 1; (b) \mathcal{D} along cluster 2; (c) Curving C along cluster 1; (d) C along cluster 2. Red curve: mean index value. Blue dashed curves: ± 1 standard deviation. Horizontal axis: arc-length parameterization s . Vertical axis: geometric index value.

Discussion The above clusters were chosen specifically for their well-defined geometric characteristics, and their expected geometry is recovered by the subsequent analysis. Due to the clusters' approximate symmetry, $s=0.5$ corresponds approx. to the intersection of the tracts with the mid-sagittal plane. As their trajectories part on either side of the mid-sagittal plane, an increase in \mathcal{D} is recorded as two peaks on either side of $s=0.5$ in Fig. 2 (a) and (b). The two peaks in Fig. 2(a) near $s=0$ and $s=1$ detect the dispersion in the tracts as they fan near the cortex. As for those near $s=0$ and $s=1$ in (b), they correspond to the strong dispersion in cluster 2 as the fibres twist towards the temporal lobes. The same geometric features are also detected by the curving index C in Fig. 2 (c) and (d), as they are also characterized by high curvature. Such parametric representations of fibre geometry are an important tool for the understanding of white matter tract structure. In future work, we will incorporate such representations in population studies of white matter abnormalities in schizophrenia.

References [1] Savadjiev, P. *et al.* MICCAI, 345-352, 2009. [2] Savadjiev, P. *et al.*, NeuroImage, In Press, 2009. [3] Kindlmann, G. *et al.* IEEE TMI 26(11):1483-1499, 2007. [4] Westin, C.-F. *et al.* Medical Image Analysis 6:93-108, 2002. [5] <http://www.slicer.org> [6] Maddah, M. *et al.* Medical Image Analysis 12(2): 191-202, 2008.

Acknowledgements Work supported by NIH grants P50MH080272, R01MH50740, R01MH074794, P41RR013218, U41RR019703, U54EB005149.